PNAS
www.pnas.org

Supplementary information for

An engineered chimeric toxin that cleaves activated mutant and wild-type RAS inhibits tumor growth

Authors: Vania Vidimar[1], Greg L. Beilhartz[4], Minyoung Park[4,5], Marco Biancucci[1‡], Matthew B. Kieffer[1§], David R. Gius[2,3], Roman A. Melnyk[4,5]*, Karla J. F. Satchell[1,3]*

Corresponding authors: Karla Satchell and Roman Melnyk

Email: k-satchell@northwestern.edu, roman.melnyk@sickkids.ca

This PDF file includes:

Supplementary Materials and Methods

Plasmids design, protein purification and endotoxin removal

DNA sequence corresponding to RRSP aa 3580-4089 was amplified from a plasmid containing the effector domain region cloned from *V. vulnificus* CMCP6 in vector pXL PCR-TOPO (1). The amplified gene was fused to different DT variants using the NEBuilder® HiFi DNA Assembly Cloning Kit (New England Biolabs Inc.). DNA sequence corresponding to CPD (nucleotides nt 12269-12894 of *rtxA1*) of MARTX toxin from *V. vulnificus* was codon-optimized and synthesized as a double-stranded DNA fragment (IDT) and inserted into the DT vector as above (2). A point mutation was made in RRSP using QuikChange Lightning Multi Site-Directed Mutagenesis Kit (Agilent Technologies) to change His4030 CAT codon to Ala (GCT) to generate the catalytically inactive $RRSP_{H4030A}$ mutant (RRSP*-DT_B). The final products were cloned into the Champion pET-SUMO expression system (Invitrogen). The different DT variants fused to RRSP were expressed as N-terminal His6-tagged and C-terminal StrepTagII-tagged proteins, transformed into either *E. coli* NiCo21(DE3) or BL21 (DE3) cells, and grown overnight in Luria-Bertani (LB) broth containing 50 µg/mL kanamycin. Next, overnight cultures were diluted 1:50 in fresh TB containing 35 µg/mL kanamycin and grown to OD_{600} = 0.8-1.0 at 37°C. Cultures were then induced with 1 mM isopropyl β-d−1-thiogalactopyranoside (IPTG) for 5 h at 25°C. Bacteria were pelleted by centrifugation at 10,000 rpm for 15 min and resuspended in 150 mL of Lysis Buffer (20 mM Tris-HCl pH 8.0, 500 mM NaCl, 20 mM imidazole, 2 mg/ml lysozyme and one tablet of EDTA-free protease inhibitor cocktail). Resuspended cells were sonicated using a Branson Digital Sonifier for 30 min (parameters: pulse ON 10 sec, pulse OFF 20 sec, 10 min, Amplitude 50%), the lysate spun down at 12,000 x g for 30 min and then loaded onto a 5 ml His-Trap Crude FF column (GE Healthcare) using a ÄKTA Purifier protein purification system (GE Healthcare). His-tagged

proteins were eluted with a buffer containing 20 mM Tris-HCl pH 8.0, 500 mM NaCl and 500 mM imidazole. Fractions corresponding to the protein peaks were collected, pooled and loaded onto a gravity column containing Strep-Tactin Superflow high capacity resin (#2-1208-025, Iba Lifesciences). Strep-tagged proteins were eluted using 20 mM Tris-HCl pH 8.0, 150 mM NaCl and 10 mM d-Desthiobiotin. The His-Sumo tag was then removed by adding 0.01 µg of Sumo protease per 100 µg of purified protein in 20 mM Tris-HCl pH 8.0, 150 mM NaCl and 1 mM dithiothreitol at 30°C for 1 h. Next, proteins were further purified by size exclusion chromatography (SEC) using the HiLoad Superdex 16/600 200 prep grade column (GE Healthcare) run in 20 mM Tris-HCl pH 8.0 and 150 mM NaCl. Proteins were then dialyzed overnight using a ThermoFisher Slide-A-lyzer cutoff 20K in 20 mM Tris-HCl pH 8.0 and 150 mM NaCl and concentrated with a Millipore Amicon Ultra 30K spin concentrator. Finally, glycerol was added to the final protein solution containing 20 mM Tris-HCl pH 8.0, 150 mM NaCl, 10 mM imidazole and 8% glycerol. Protein purity was assessed by SDS-PAGE/Coomassie blue staining and concentration determined using NanoDrop ND1000 Spectrophotometer. Protein aliquots were flash frozen and stored at -80°C until use. For *in vivo* applications, endotoxin was removed from all protein preparations using Pierce High-Capacity Endotoxin Removal Resin (#88270) and residual endotoxin was quantified using Pierce LAL Chromogenic Endotoxin Quantitation Kit (#88282) following manufacturer's instructions (Thermo Scientific).

Cell culture and chemicals

All cell lines were purchased from the American Type Culture Collection, except for the *KRAS*^{WT}-expressing RAS-less MEF cells that were kindly provided by the RAS Initiative at Frederick National Laboratory for Cancer Research (FNLCR) (Designation RPZ26216, expressed transgene

KRAS 4B WT) (3). Cells were cultured at 37°C and 5% CO_2 atmosphere. MDA-MB-436, MDA-MB-231 and HCT-116 were grown in DMEM-F12 with Glutamax (Gibco) containing 10% fetal bovine serum (FBS; Gemini) and 1% penicillin/streptomycin (P/S; Invitrogen). Hs578T were grown in DMEM containing 10% FBS and 1% P/S (complete DMEM). MEF cells were cultured in complete DMEM with 4 μg/ml of blasticidin. All chemicals, unless otherwise specified, were purchased for Sigma-Aldrich.

Antibodies

The anti-RAS 4E8 hybridoma cell line was kindly provided by the Frederick National Laboratory for Cancer Research (FNLCR). The antibody was purified by affinity chromatography as described in (4). Antibody validation was performed as follows. 10 μM of recombinant K-, N- or H-RAS proteins were incubated alone or together with 1 μM of recombinant RRSP for 5 minutes at room temperature and then 1 μg of each sample was run on an SDS-PAGE gel followed by western blotting. The purified antibody used at 1:2000 dilution specifically recognized both cleaved and uncleaved bands of all three RAS isoforms (Fig. S2I). This antibody thus is a pan-RAS monoclonal, here designated as mAb 4E8.

Some western blots and immunohistochemistry were performed with the commercially available anti-panRAS (Ras10, MA1-012; Thermo Fisher Scientific) antibody, that recognizes RAS Switch I and thus detects only uncleaved RAS. Other primary antibodies used are anti–Phospho-p44/42 MAPK (phosphorylated ERK1/2, Thr202/Tyr204, 197G2, Cell Signaling Technology #4377), anti-p44/42 MAPK (ERK1/2, L34F12, Cell Signaling Technology #4696), anti-HB-EGF (R&D Systems, #AF-259-NA;), and precision protein StrepTactin-HRP Conjugate rabbit Bio-Rad (#1610381) The anti-vinculin (Cell Signaling Technology #13901) was used for

normalization. Secondary antibodies used were fluorescent-labeled IRDye 680RD goat anti-mouse (926-68070), IRDye 800CW goat anti-rabbit (925-322211) and IRDye 800CW donkey anti-goat (925-32214) from LI-COR Biosciences. Blot images were acquired using an Odyssey Infrared Imaging System (LI-COR Biosciences) and quantified by densitometry using NIH ImageJ software. Percentage of uncleaved RAS was calculated as previously described (5).

SDS-PAGE and Western Blotting

At the experimental endpoint, cells were washed once with ice-cold PBS and protein lysates were extracted using M-PER mammalian protein extraction reagent (Thermo Fisher Scientific) with protease and phosphatase inhibitors (Sigma-Aldrich). Protein concentration was quantified using Bio-Rad protein assay dye reagent concentrate (#5000006). Equal amounts of proteins were separated by SDS-PAGE followed by western blot analysis as previously described (5).

Cell viability, proliferation and growth inhibition assays

For quantitative viability assays, 10,000 cells per well were cultured in 96-well clear bottom white plates in the corresponding complete growth medium and treated the next day with RRSP-DT_B and RRSP*-DT_B. At the end of treatments, CellTiter-Glo (Promega) was added to each well according to the manufacturer's manual and luminescence was acquired using a Tecan Safire2 plate reader. CellTiter-Glo was incompatible with assessment of MDA-MB-436 cell viability under the experimental conditions used. Indeed, despite the cells being very sensitive to RRSP-DT_B, no change in luminescence were detected between untreated and treated cells presumably due to release of ATP to the media that complicates the CellTiter-Glo reaction. Therefore, for this

cell line, viability was determined via crystal violet assay. Briefly, MDA-MB-436 cells (10,000 cells/well) were plated in 96-well plates and treated with RRSP-DT_B and RRSP*-DT_B. At the experimental endpoint, medium was carefully removed and cells gently washed with PBS. Crystal violet fixing/staining solution (0.05% (g/vol) crystal violet, 1% formaldehyde, 1% (v/v) methanol in phosphate buffered saline (PBS)) was then added to each well and the plate incubated at room temperature for 20 min. Next, wells were washed with tap water, air-dried, crystal violet solubilized using 10% acetic acid and absorbance recorded at 570 nm using a Tecan Safire2 plate reader. IC_{50} were calculated using the log(inhibitor) vs. response - variable slope (four parameters) function in Graphpad Prism. Crystal violet assay was also performed to visually assess viability of adherent cells using the same procedure described above but instead of solubilizing the dye, images of 6-well air-dried plates were acquired using a conventional desktop scanner. Cell proliferation was measured by colony-formation assay. Cells were treated with RRSP-DT_B and 10 nM RRSP*-DTB. After 72 hours, cells were harvested by trypsinization, counted on a hemocytometer and replated in 6-well plates at 2,500 cells per well. Colony formation was monitored over 10 days period, during which medium was replaced every two days. On day 10, crystal violet was applied to visualize the colonies. The open source ColonyArea ImageJ plug-in was used for quantitative analysis of the area % covered by the stained colonies (6). Quantification of cell rounding was carried out by manually counting up to 200 rounded cells (with sharp edges and no protrusions) per image and means ± SD of three independent experiments were plotted. Because all cells treated with 10 nM of RRSP-DT_B appeared round, this condition was set as 100% cell roundness.

An NCI-60 five dose growth inhibition screen was performed on a panel of 60 human tumor cell lines derived from nine different tumor types by the National Cancer Institute Developmental Therapeutics Program (NCI-DTP) and growth inhibition percentage was

calculated in accordance with their standard protocol previously published (7). We normalized all data such that 0% growth inhibition corresponded to no change in the cell number relative to control after 48 hours of treatment with the high dose of RRSP-DT_B (13.5 nM), while a drop of 100% corresponded to no cell growth relative to time zero (100% growth inhibition); values below 100% correspond to cell loss. Additional information about the screening methodology can be found on the NCI-DTP website (8).

Maximum tolerated dose (MTD) and xenograft studies

The MTD study was performed at Charles River Laboratories (Wilmington, MA). Both female and male athymic NU(NCr)-*Foxn1*^{nu} mice were used (5 mice/group). Mice received increasing dosing of RRSP-DT_B (0.004, 0.02, 0.1 and 0.5 mg/kg) and RRSP*-DT_B (0.5 mg/kg) via IP injection on an everyday schedule – weekends excluded – for two weeks. Mouse weight was monitored on a regular basis until the end of the experiment. Mice were humanely euthanized after loss of 20% body weight and counted as non-survivors.

MDA-MB-436 and MDA-MB-231 mouse xenografts were performed following our animal protocol, which was approved by the Institutional Animal Care and Use Committee (IACUC) at Northwestern University. Mice were maintained in Allentown cages in a sterile housing facility under controlled environmental conditions. 5-week old athymic NU(NCr)-*Foxn1*^{nu} female mice were injected subcutaneously with $2.5x10^6$ cells in 100 µl/mouse of 50% 1X endotoxin-free PBS/50% Matrigel (Corning #356237) onto the right flank under anesthesia. On day 7, when tumors reached 100-200 mm^3 in size, mice were randomized into groups of 5 and treatment started. For the MDA-MB-436 xenograft, control mice were administered IP with saline (endotoxin-free PBS) and treatment groups with 0.1 mg/kg of RRSP-DT_B and 0.1 mg/kg of

RRSP*-DT_B on an every-other-day schedule (weekends excluded) for about 4 weeks. In a second experiment with the same cell line, mice were treated with 0.1 mg/kg of RRSP-DT_B every other day (EOD) and 0.1 mg/kg of RRSP-DT_B every day (ED) for about 4 weeks as well as with 0.25 mg/kg of RRSP-DT_B for two weeks followed by 0.1 mg/kg RRSP-DT_B for additional two weeks (weekends excluded). For the MDA-MB-231 xenograft, mice were treated with 0.1 mg/kg of RRSP-DT_B and 0.1 mg/kg of RRSP*-DT_B on an ED schedule (weekends excluded) for 4 weeks. Tumor size was measured twice a week using a digital caliper and tumor volume was calculated using the following formula: volume (mm^3) = (l x w^2)/2, where l is the length and w the width of the tumor. Mouse body weight was also measured twice a week.

The HCT-116 xenograft study was performed at Charles River Laboratories (Wilmington, MA). 5 x 10^6 cells in 100 µl PBS (no Matrigel) were inoculated into the right flank of athymic NU(NCr)-*Foxn1*^{nu} female mice. When tumors reached an average size of 80 - 120 mm^3, mice were randomized into 5 groups of 10 and treatment started. The first group received PBS (saline), the second 0.1 mg/kg of RRSP-DT_B every day (1X/day), the third 0.1 mg/kg of RRSP-DT_B twice per day (2X/day), the fourth 0.1 mg/kg of RRSP*-DT_B 1X/day and the fifth 0.1 mg/kg of RRSP*-DT_B 2X /day. Both tumor size and mouse body weight were measured biweekly. For all the *in vivo* experiments performed in this study, when tumors exceeded 1500 mm^3, mice were sacrificed as per protocol. At the end of the treatment schedule, mice were euthanized, tumors excised, and fixed in 10% formalin overnight.

Spheroid formation, viability and image analysis

For tumor spheroids generation, a single cell suspension of HCT-116 cells was seeded at a concentration of 10,000 cells/well into 96-well ultra-low attachment plates (Corning #4520) in

complete medium. Two days after cell seeding, treatments were added and viability assessed after 1, 3, 5 and 7 days using the Promega CellTiter-Glo 3D Cell Viability Assay following the manufacturer's protocol. Spheroids were imaged at every time point with an EVOS XL Core imaging system and their volume analyzed using a freely available ImageJ plug-in as described in (9). Spheroids fixation and agarose-embedding prior to immunohistochemical analysis was performed as previously described (10).

Immunohistochemistry of spheroids and *in vivo* tumors

Spheroids as well as *in vivo* tumors processing, paraffin-embedding, sectioning and immunohistochemical stainings were performed by the Robert H. Lurie Comprehensive Cancer Center's Pathology Core Facility. Anti-rabbit pan-Ras (#PA5-85947; Thermo Fisher Scientific) and anti-rabbit Phospho-p44/42 MAPK (Erk1/2) (Thr202/Tyr204, (D13.14.4E) XP Cell Signaling #4370) antibodies were used at 1:500 and 1:300 dilutions, respectively. Primary antibodies were detected using a standard anti-rabbit secondary antibody followed by 3,3′-diaminobenzidine (DAB) revelation (Dako). Quantification of immunohistochemical signal intensity was performed by color deconvolution using ImageJ (Fiji version) as previously described (10).

Bioinformatic analysis

Bioinformatics analyses were performed using R version 3.5.2. NCI-60 mutation data were retrieved from Reinhold WC et al (11). For the A549/ATCC and MDA-MB-231/ATCC cell lines, mutations were obtained from the ATCC website (https://www.atcc.org/~/media/PDFs/Culture%20Guides/Cell_Lines_by_Gene_Mutation.ashx). NCI-60 gene copy number alteration data and RNA expression z-scores were downloaded from

cBioPortal (https://www.cbioportal.org) for the study with id "cellline_nci60" using the TCGAretriever R package (https://cran.r-project.org/web/packages/TCGAretriever/index.html). Bar plots, tile plots, and violin plots were built using ggplot2.

Statistics

Statistical analysis was performed using Graphpad Prism software v.8. Bar plots represent mean of at least three independent experiments ± the standard deviation (SD). Statistical significance was determined using one-way analysis of variance (one-way ANOVA) assuming normal distribution. Dunnett's multiple comparison post-test was used to compare the mean of treatment groups to the mean of the control group and Tukey's multiple comparison test was used to compare the mean of each group with the mean of every other group. Points in the fitted dose-response curve are mean ± standard error of the mean (SEM). Statistical analysis on fold change data was carried out after log transformation of the data to obtain a more normalized distribution. For *in vivo* xenografts, data are reported as mean ± SEM and one-way ANOVA was performed to test for differences among the groups. Values of $p<0.05$ were considered statistically significant.

Supplementary Results

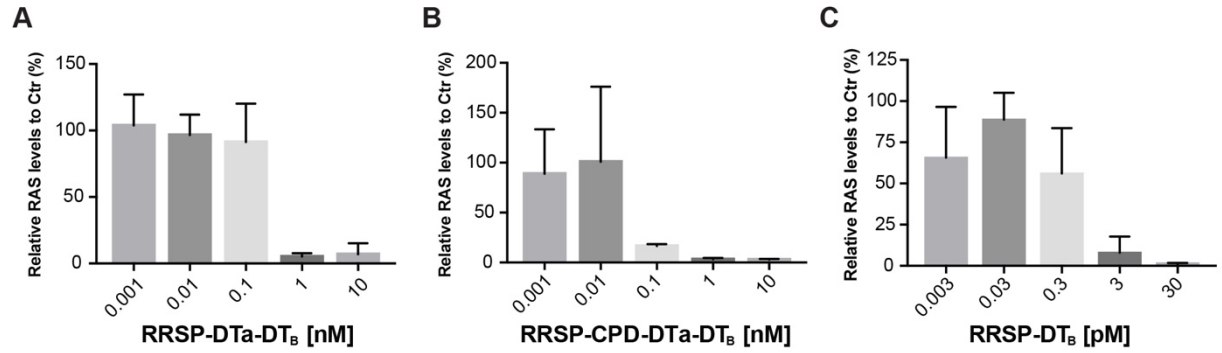

Fig. S1. Densitometric analysis showing the effect of various RRSP chimeras on total RAS levels in HCT-116 cells. Densitometric analysis of western blots from HCT-116 cells (*KRAS*^{G13D}) treated with the indicated amount of various RRSP chimeras. (A) RRSP-DTa-DT$_B$ is RRSP fused to a detoxified mutant DT (K51E/E148K) (DTa) via a (Gly-Gly-Gly-Gly-Ser)X2 ((G4S)2) linker. (B) RRSP-CPD-DTa-DT$_B$ is RRSP fused to the cysteine protease domain (CPD) of the *V. vulnificus* MARTX toxin as in (A). (C) RRSP-DT$_B$ is RRSP fused directly to DT residues 186-535 via a (G4S)2 linker.

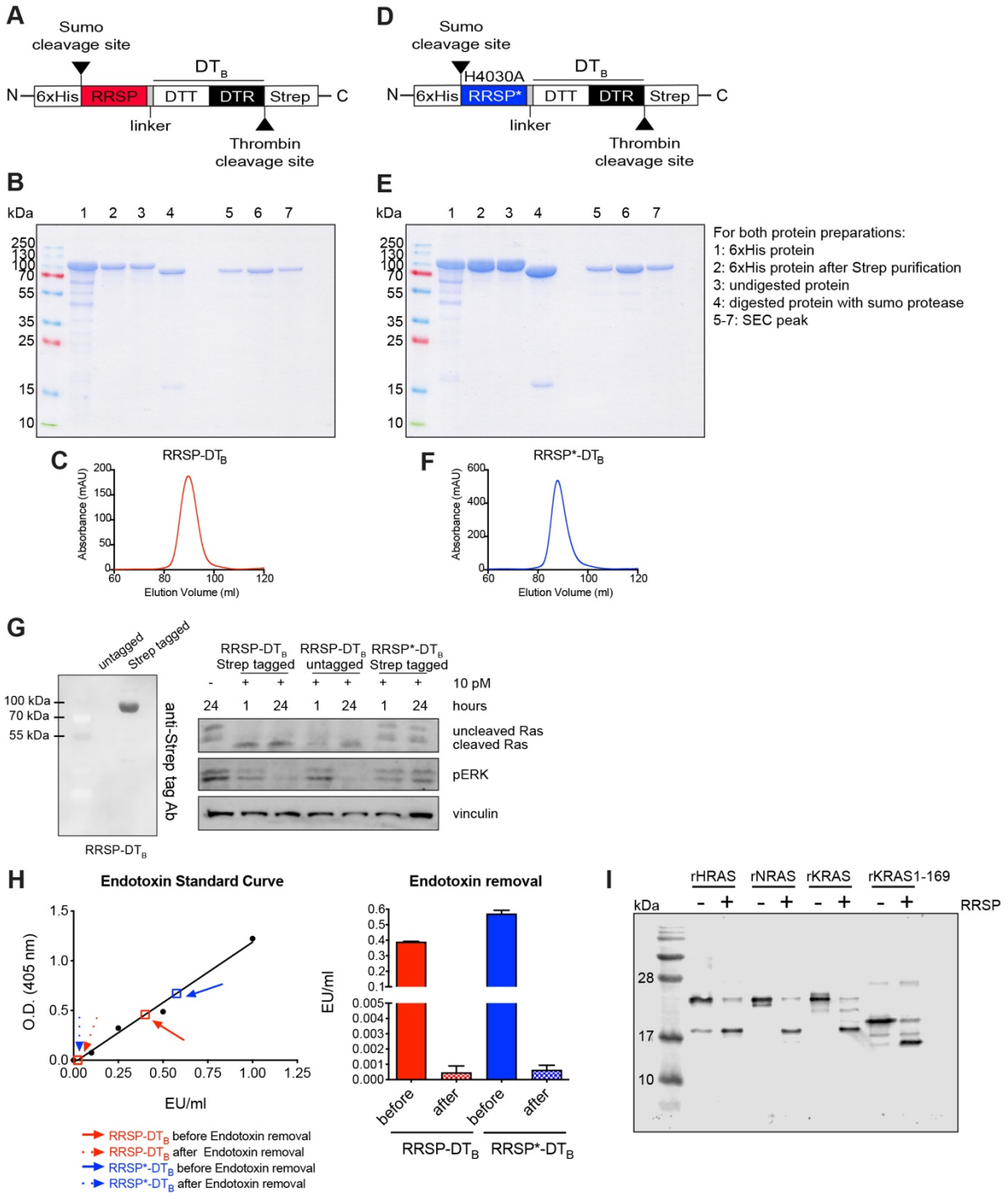

Fig. S2. Purification of RRSP-DT$_B$ and RRSP*-DT$_B$ proteins and validation of panRAS antibody for detection of uncleaved/cleaved RAS. (A, D) Schematic representation of RRSP-DT$_B$ (A) and RRSP*-DT$_B$ (D) plasmid constructs. (B, E). Coomassie gel images of RRSP-DT$_B$

(B) and RRSP*-DT_B (E) proteins showing degree of protein purity after nickel affinity purification, Strep-purification, removal of the SUMO-tag and size exclusion chromatography (SEC). (C, F). SEC peaks of purified RRSP-DT_B (C) and RRSP*-DT_B (F). (G) Left, western blot indicating presence of the Strep-tag in the RRSP-DT_B purified protein. Right, western blot showing the effect of Strep-tagged and untagged RRSP-DT_B on RAS processing and phosphorylated ERK in HCT-116 cells. Cells were treated with 10 pM of RRSP-DT_B for 1 and 24 hours. Strep-tagged RRSP*-DT_B was also used as negative control. (H) Standard curve displaying efficiency in endotoxin removal from RRSP-DT_B and RRSP*-DT_B protein preparations for *in vivo* applications. Bar plots show residual endotoxin content (expressed in EU/ml) in both RRSP-DT_B and RRSP*-DT_B protein preparations. (I) Western blot image showing validation of the purified pan-RAS antibody used for detection of uncleaved/cleaved RAS. Recombinant HRAS, NRAS and KRAS were incubated with or without recombinant RRSP and samples were run on a SDS-PAGE gel followed by western blotting. The antibody recognized both cleaved and uncleaved bands of all RAS isoforms.

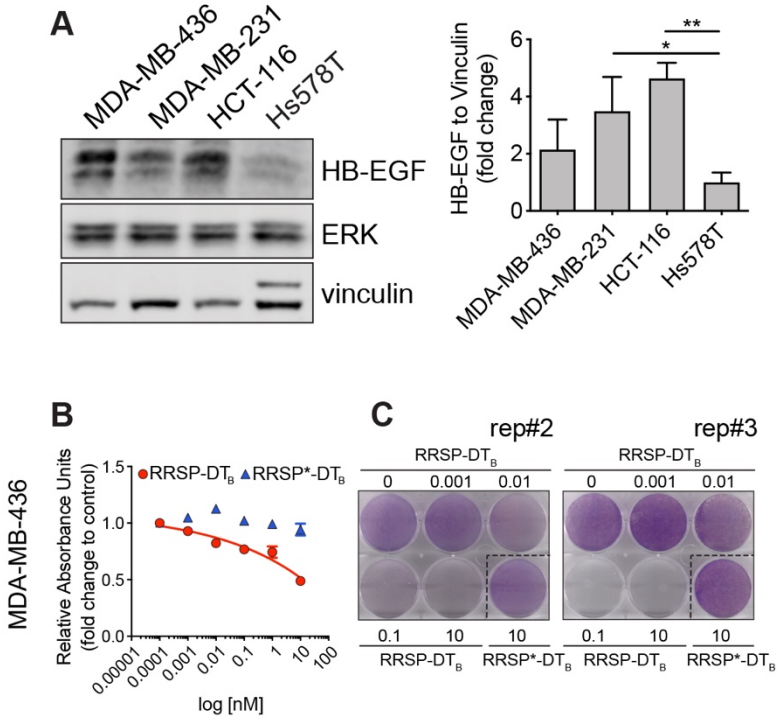

Fig. S3. HB-EFG protein levels and additional data on the effect of RRSP-DT$_B$ on viability of MDA-MB-436. (A) Western blot image and densitometry showing expression of the DT receptor HB-EGF across MDA-MB-436, MDA-MB-231, HCT-116 and Hs578T cell lines. (B) Dose-response curve of RRSP-DT$_B$ in MDA-MB-436 cells following 24 h of treatment. Slopes of the dose-response curves for both RRSP-DT$_B$ and mutant RRSP*-DT$_B$ were not steep enough to retrieve an IC$_{50}$. Results are expressed as means ± SEM (n=3). (C) Additional two replicate images of crystal violet staining of MDA-MB-436 cells treated for 72 h with RRSP-DT$_B$ and RRSP*-DT$_B$ as indicated.

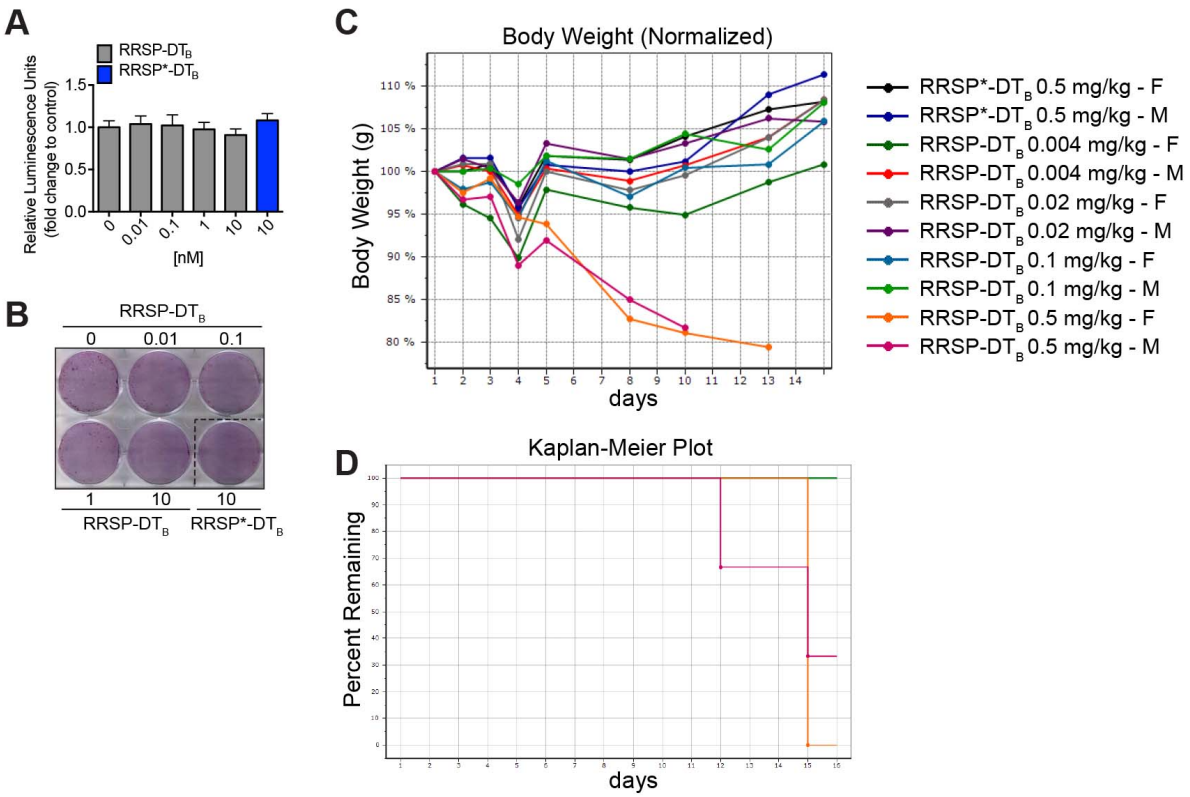

Fig. S4. Effect of RRSP-DT$_B$ on mouse embryonic fibroblasts (MEF) and *in vivo* Maximum Tolerated Dose (MTD) study. (A) Viability and (B) crystal violet staining of RAS-less *KRAS*^{WT} MEF cells following 72 h of treatment with RRSP-DT$_B$ and RRSP*-DT$_B$ as indicated. (C) Body weight expressed as percentage of initial weight over time from the MTD study that was performed treating athymic female *nu/nu* nude mice at the indicated doses every day for two weeks (weekends excluded, F=female, M=male). (D) Kaplan-Meier plot showing overall survival of mice treated with RRSP-DT$_B$ and RRSP*-DT$_B$.

A MDA-MB-436 - Total Ras_4 weeks

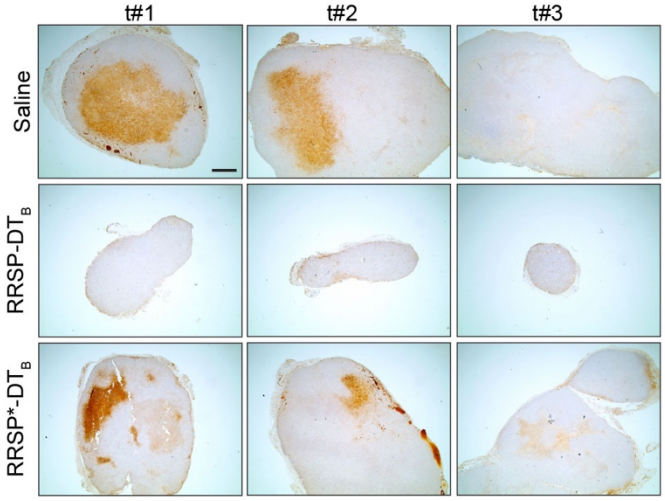

B MDA-MB-436 - pERK_4 weeks

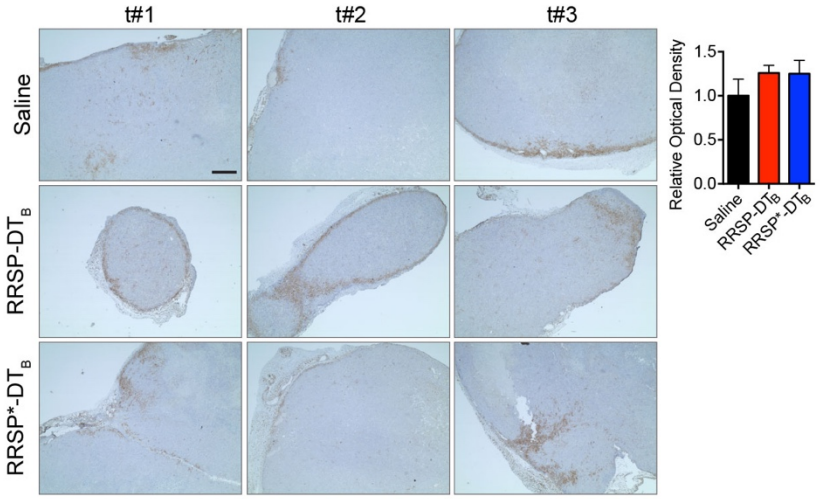

C MDA-MB-436 - pERK_2 weeks

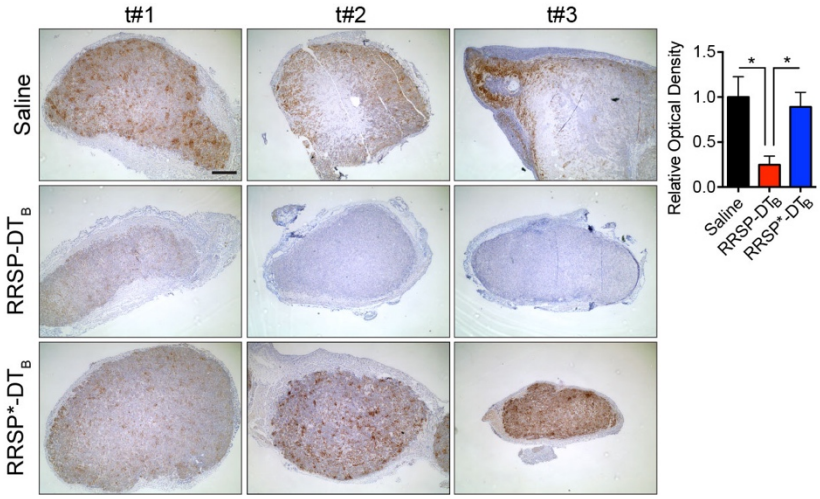

Fig. S5. Whole tumor IHC images and analysis of total RAS and pERK levels from the MDA-MB-436 xenograft. (A) Sections of whole tumors from the MDA-MB-436 xenograft immunostained with a total RAS antibody (n = 3; scale bar = 200 μm). Mice were treated every other day (weekends excluded) at the indicated treatment conditions for about 4 weeks. (B) Sections of whole tumors from the same MDA-MB-436 xenograft immunostained with a pERK antibody (scale bar = 100 μm). Bar plot shows quantification of pERK DAB signal (n = 3). (C). Sections of whole tumors from a shorter, 2-week long MDA-MB-436 xenograft immunostained with a pERK antibody and quantification of DAB signal (*$p < 0.05$, one-way ANOVA followed by Tukey's multiple comparison test, n=3; scale bar = 200 μM).

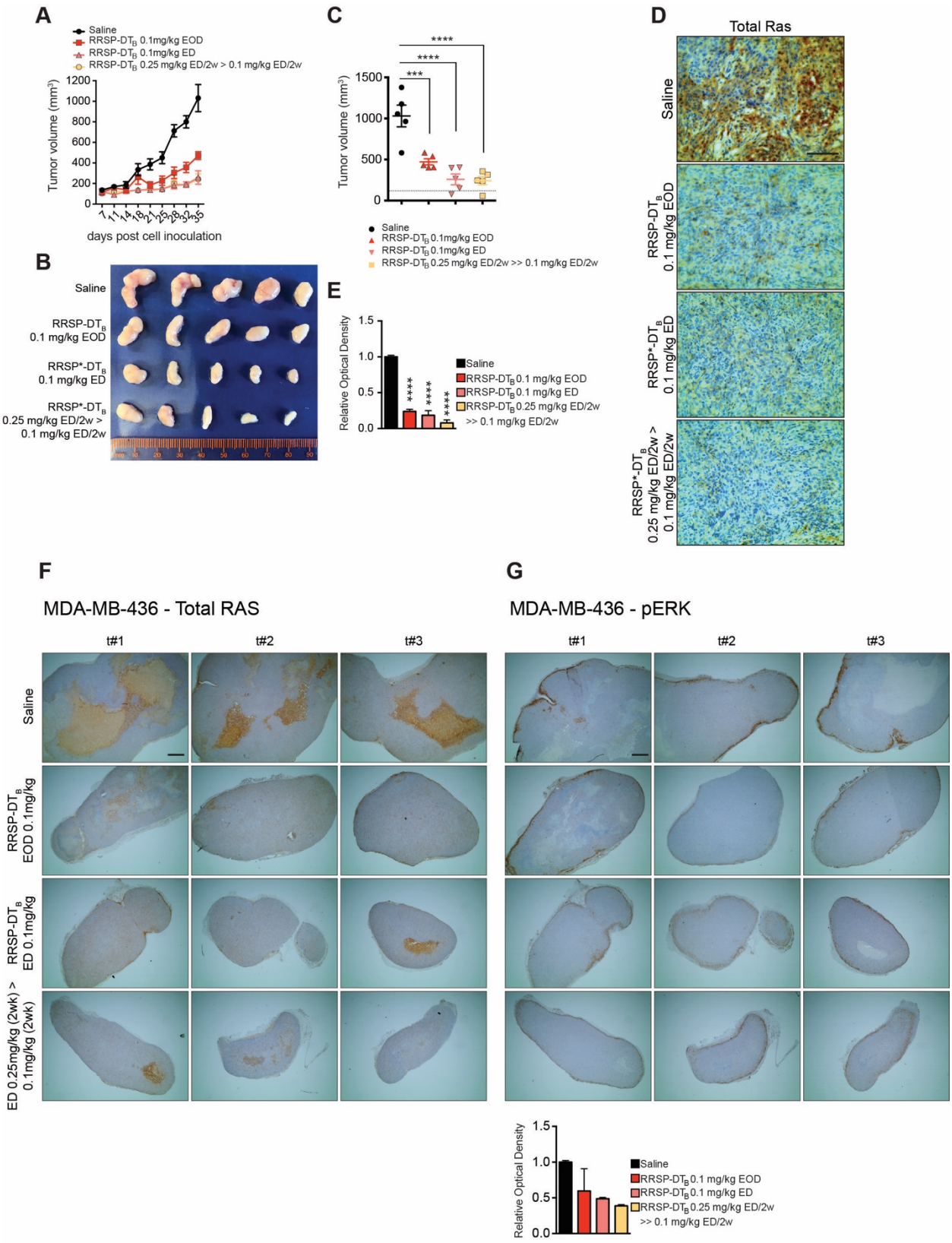
A
Saline
RRSP-DTB 0.1mg/kg EOD
RRSP-DTB 0.1mg/kg ED
RRSP-DTB 0.25 mg/kg ED/2w > 0.1 mg/kg ED/2w
Tumor volume (mm3)
days post cell inoculation
B
Saline
RRSP-DTB 0.1 mg/kg EOD
RRSP*-DTB 0.1 mg/kg ED
RRSP*-DTB 0.25 mg/kg ED/2w > 0.1 mg/kg ED/2w
C
Tumor volume (mm3)
Saline
RRSP-DTB 0.1mg/kg EOD
RRSP-DTB 0.1mg/kg ED
RRSP-DTB 0.25 mg/kg ED/2w >> 0.1 mg/kg ED/2w
D
Total Ras
Saline
RRSP-DTB 0.1 mg/kg EOD
RRSP*-DTB 0.1 mg/kg ED
RRSP*-DTB 0.25 mg/kg ED/2w > 0.1 mg/kg ED/2w
E
Relative Optical Density
Saline
RRSP-DTB 0.1 mg/kg EOD
RRSP-DTB 0.1 mg/kg ED
RRSP-DTB 0.25 mg/kg ED/2w >> 0.1 mg/kg ED/2w
F
MDA-MB-436 - Total RAS
t#1
t#2
t#3
Saline
RRSP-DTB EOD 0.1mg/kg
RRSP-DTB ED 0.1mg/kg
ED 0.25mg/kg (2wk) > 0.1mg/kg (2wk)
G
MDA-MB-436 - pERK
t#1
t#2
t#3
Relative Optical Density
Saline
RRSP-DTB 0.1 mg/kg EOD
RRSP-DTB 0.1 mg/kg ED
RRSP-DTB 0.25 mg/kg ED/2w >> 0.1 mg/kg ED/2w

Fig. S6. Summary of the effect of RRSP-DT$_B$ on an additional MDA-MB-436 xenograft. (A) Tumor growth curve of vehicle and RRSP-DT$_B$-treated athymic *nu/nu* female mice bearing MDA-MB-436 tumors at the indicated doses and treatment schedule. EOD, every other day. ED, every day. (B) Representative images of MDA-MB-436 tumors at the experimental endpoint. (C) Column scatter plots showing individual tumor volumes at the end of the treatment schedule. Horizontal dashed lines indicate the baseline tumor volume on the first day of treatment, which corresponds to the average of tumor volumes at the indicated time (118 mm^3). Data are means ± SEM and n=5 mice in every group. Statistical analysis between vehicle and treatment groups was performed using one-way ANOVA followed by Tukey's multiple comparison test (***$p < 0.001$, ****$p < 0.0001$). (D) Representative IHC images of immunoreactivity to total RAS in sections from MDA-MB-436 tumors and (E) corresponding quantification of DAB optical density (****$p < 0.0001$, one-way ANOVA followed by Tukey's multiple comparison test, n=3; scale bar = 100 μM). (F). Sections of whole tumors from the MDA-MB-436 xenograft immunostained with a total RAS antibody and (G) pERK antibody (n = 3; scale bar = 200 μm). Bar plot shows quantification of pERK DAB signal.

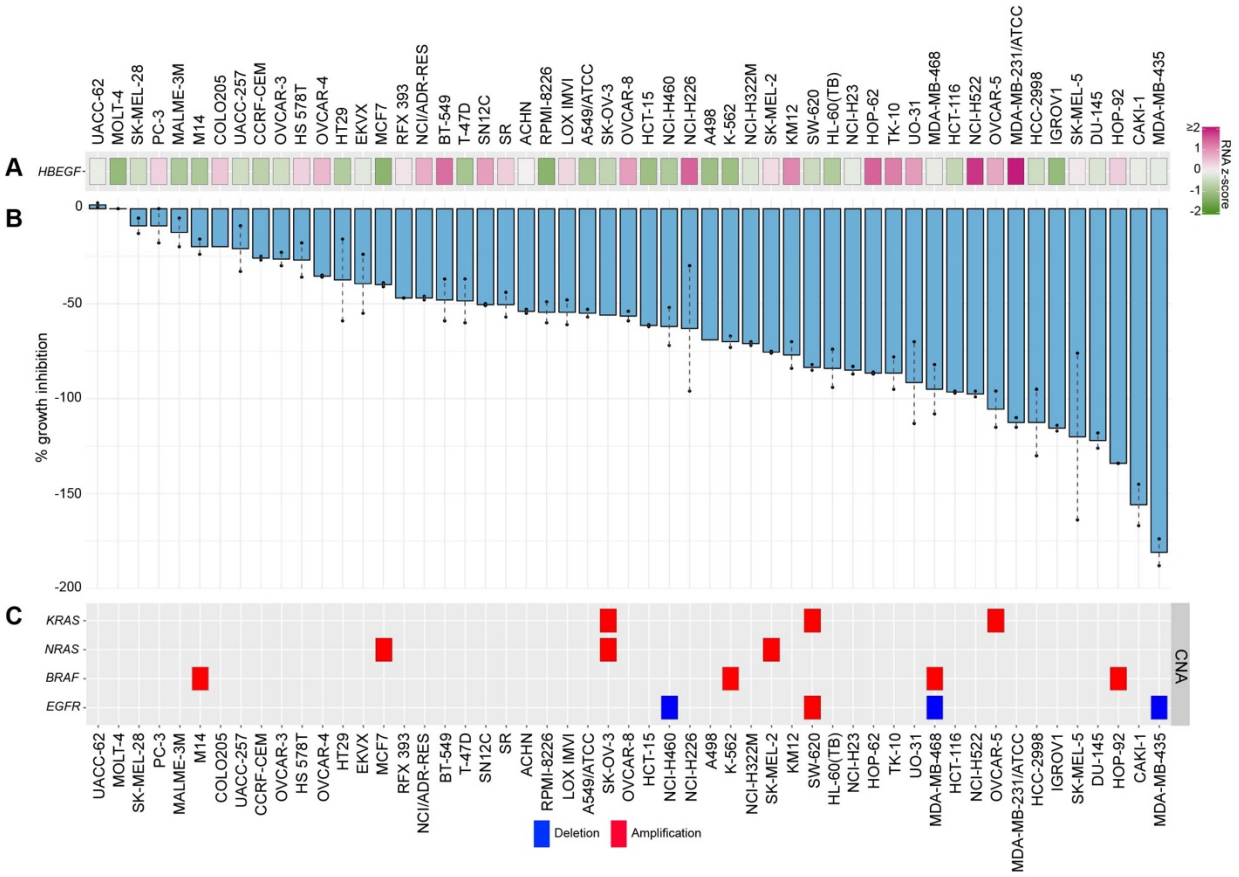

Fig. S7. Expression of HB-EGF and copy number alterations of *KRAS, NRAS, BRAF* and *EGFR* across several cell lines from the NCI-60 panel. (A). Heatmap of RNA-Seq expression z-scores for human HB-EGF in 53 out of 60 cell lines included in the NCI-60 panel. Data were retrieved from cBioPortal (https://www.cbioportal.org) for the study with id "cellline_nci60". The color key indicates gene expression value (pink for upregulated and green for downregulated). (B). Bar plot showing the percent growth inhibition of RRSP-DT_B for the 56 cell lines included in the analysis. Cancer cell lines were ranked in descending order based on their growth inhibition % value. The presence of two dots on the bars indicate that two replicates were performed per each cell line and bars represent means. No dots indicate that only one replicate was available. (C). Map of copy number alterations in *KRAS, NRAS, BRAF* and *EGFR* genes across the 53 cell lines from the NCI-60 panel. Red indicates gene amplification and blue gene deletions.

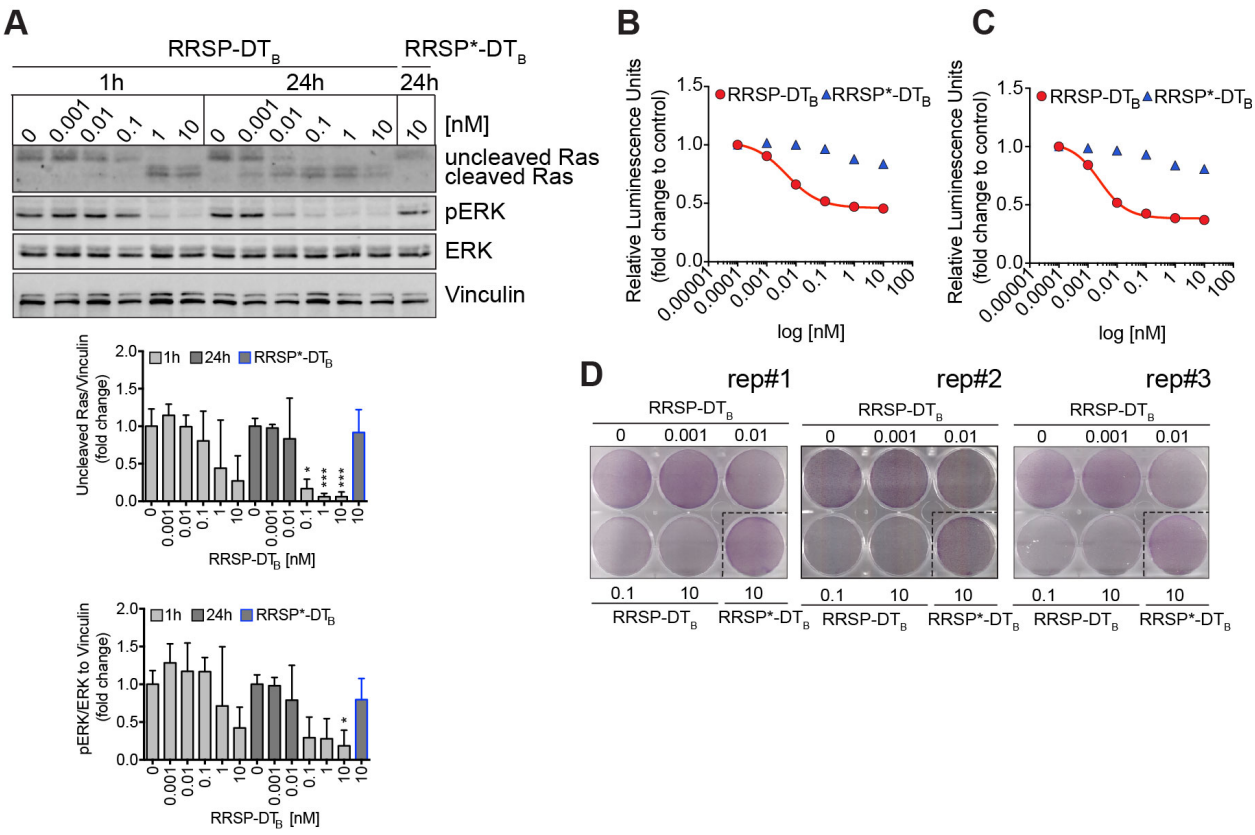

Fig. S8. Effect of RRSP-DT$_B$ on the TNBC Hs578T *HRAS*^{G12D} cell line. (A). Representative western blot and densitometric analysis of uncleaved RAS and phosphorylated ERK in Hs578T *HRAS*^{G12D} cells treated with increasing doses of RRSP-DT$_B$ for 1 and 24 h. The catalytically-inactive RRSP*-DT$_B$ mutant was used as negative control at 10 nM and vinculin as gel loading control. Results are expressed as means ± SD of three independent experiments (*$p < 0.05$, ***$p < 0.001$ versus corresponding control 0 nM; one-way ANOVA followed by Dunnett's multiple comparison test, n = 3). (B and C) Fitted dose-response curve of RRSP-DT$_B$ in Hs578T cells following 24 (B) and (C) 72 h of treatment. Slopes of the dose-response curves for both RRSP-DT$_B$ and mutant RRSP*-DT$_B$ were not steep enough to retrieve an IC$_{50}$. Results are expressed as means ± SEM (n=3). (D). Images of crystal violet-stained plates in triplicate of Hs578T cells treated with RRSP-DT$_B$ and RRSP*-DT$_B$ as indicated for 72 h.

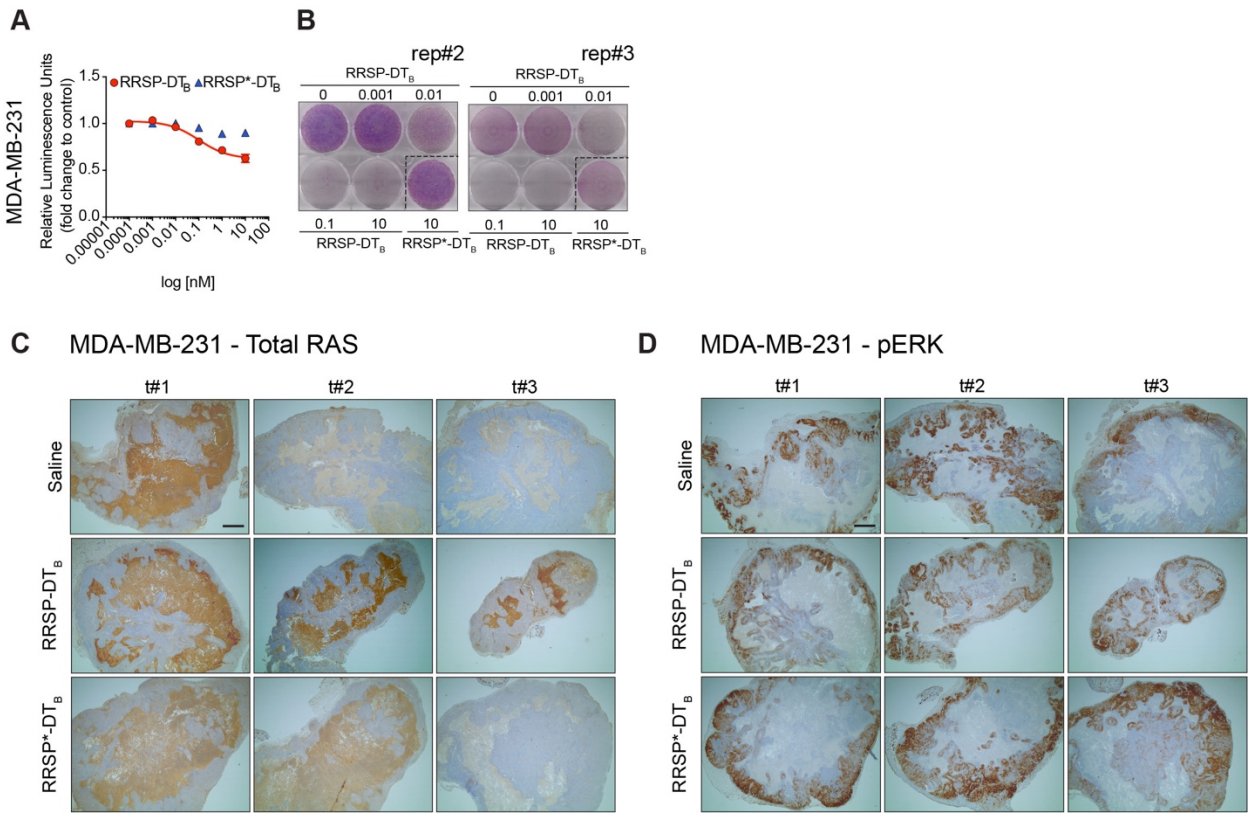

Fig. S9. Additional data on the effect of RRSP-DT$_B$ on viability of MDA-MB-231 cells and whole tumor IHC images and analysis of total RAS and phosphorylated ERK from the MDA-MB-231 xenograft. (A). Dose-response curve of RRSP-DT$_B$ in MDA-MB-231 cells following 24 h of treatment. Slopes of the dose-response curves for both RRSP-DT$_B$ and mutant RRSP*-DT$_B$ were not steep enough to retrieve an IC$_{50}$. Results are expressed as means ± SEM (*n*=3). (B) Additional two replicate images of crystal violet staining of MDA-MB-231 cells treated with RRSP-DT$_B$ and RRSP*-DT$_B$ as indicated for 72 h. (C) Sections of whole tumors from the MDA-MB-231 xenograft immunostained with a total RAS antibody (n = 3; scale bar = 200 µm). Mice were treated every day (weekends excluded) at the indicated treatment conditions for about 4 weeks. (D) Sections of whole tumors from the same MDA-MB-231 xenograft immunostained with a pERK antibody (scale bar = 200 µm).

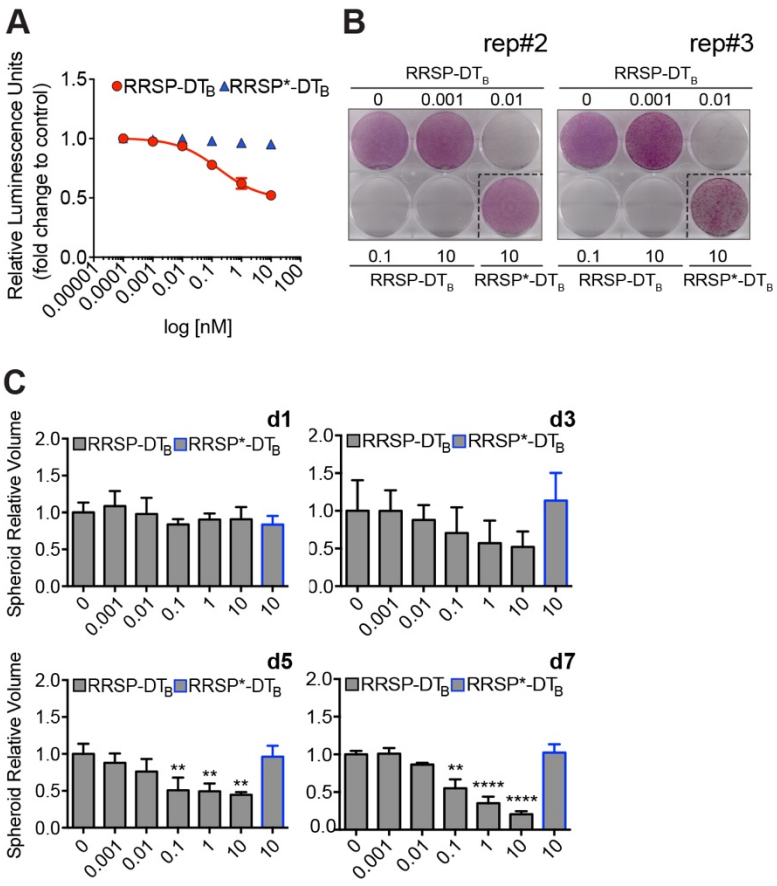

Fig. S10. Effect of RRSP-DT$_B$ on viability of CRC HCT-116 *KRAS G13D* cells after 24 hours of treatment and spheroid volume quantification. (A) Dose-response curve of RRSP-DT$_B$ in HCT-116 cells following 24 h of treatment. Slopes of the dose-response curves for both RRSP-DT$_B$ and mutant RRSP*-DT$_B$ were not steep enough to retrieve an IC$_{50}$. Results are expressed as means ± SEM (*n*=3). (B) Additional two replicate images of crystal violet staining of HCT-116 cells treated with RRSP-DT$_B$ or RRSP*-DT$_B$ as indicated for 72 h. (C). Quantitative analysis of spheroids' volumes. Results are expressed as means ± SD of three independent experiments (**p < 0.01, ****p < 0.0001 versus corresponding control 0 nM; one-way ANOVA followed by Dunnett's multiple comparison test, n = 3; d=day).

A

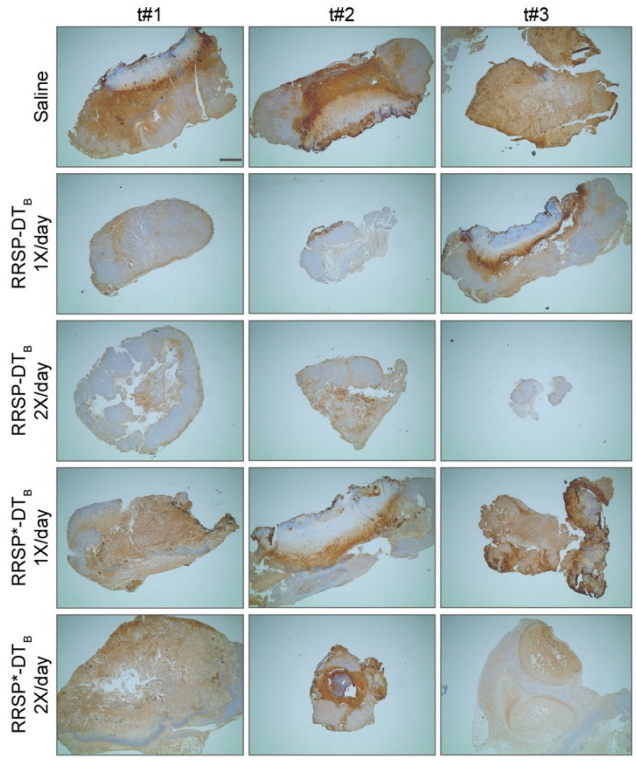
HCT-116 - Total RAS
t#1
t#2
t#3
Saline
RRSP-DT$_B$ 1X/day
RRSP-DT$_B$ 2X/day
RRSP*-DT$_B$ 1X/day
RRSP*-DT$_B$ 2X/day

B

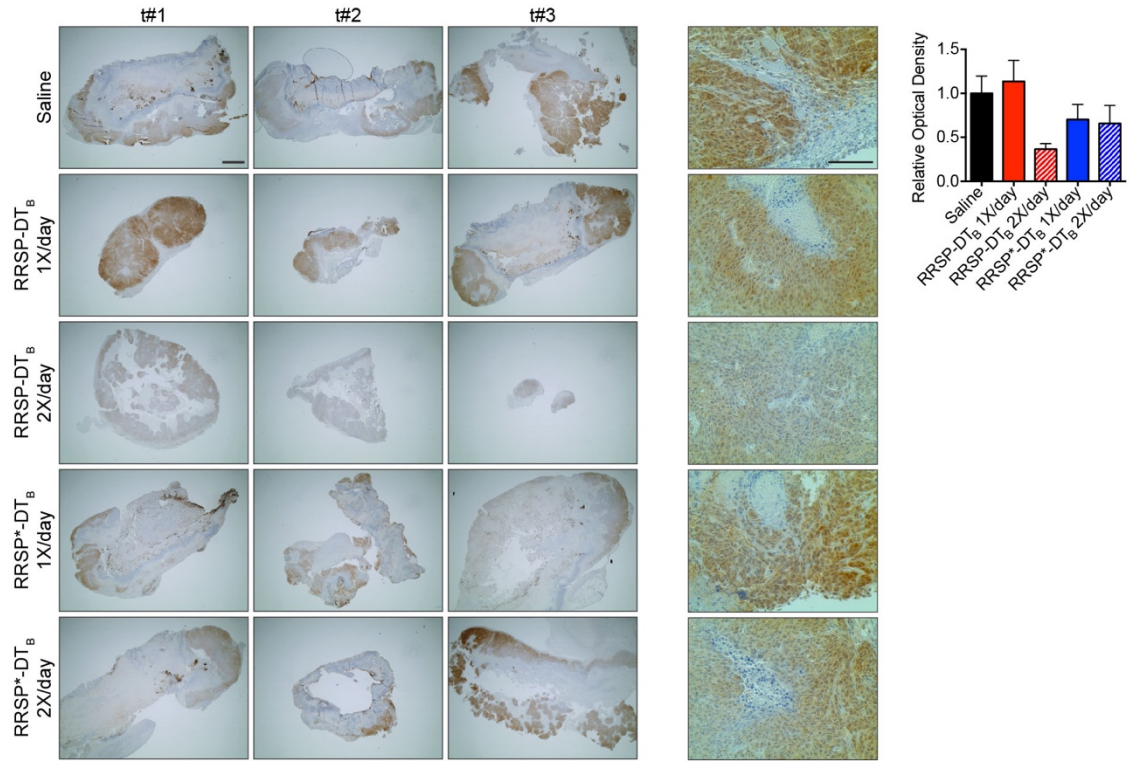
HCT-116 - pERK
t#1
t#2
t#3
Saline
RRSP-DT$_B$ 1X/day
RRSP-DT$_B$ 2X/day
RRSP*-DT$_B$ 1X/day
RRSP*-DT$_B$ 2X/day
Relative Optical Density
1.5
1.0
0.5
0.0
Saline
RRSP-DT$_B$ 1X/day
RRSP-DT$_B$ 2X/day
RRSP*-DT$_B$ 1X/day
RRSP*-DT$_B$ 2X/day

Fig. S11. Whole tumor IHC images and analysis of total RAS and phosphorylated ERK from the HCT-116 xenograft. (A) Sections of whole tumors from the same HCT-116 xenograft immunostained for phosphorylated ERK (scale bar = 200 μm). Bar plot shows quantification of pERK DAB signal (n = 3). (B) Sections of whole tumors from the HCT-116 xenograft immunostained with a total RAS antibody (n = 3; scale bar = 200 μm, left panel; scale bar = 100 μm, right panel). Mice were treated every day (1X/day) and twice per day (2X/day) weekends excluded at the indicated treatment conditions for about 4 weeks.

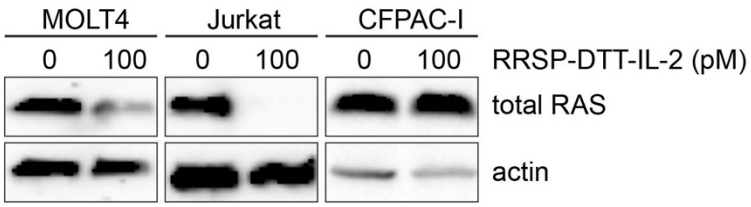

Fig. S12. Selective targeting of RRSP-DT$_B$ to IL-2 expressing cancer cells via replacement of the DTR domain. Western blot image showing total RAS levels following treatment with RRSP-DTT-IL-2 of lymphoblast MOLT4 and Jurkat cells expressing high levels of IL-2 receptor and pancreatic CFPAC-I cells expressing none to low levels of the IL-2 receptor.

SI References

1. J. S. Kwak, H. G. Jeong, K. J. Satchell, Vibrio vulnificus rtxA1 gene recombination generates toxin variants with altered potency during intestinal infection. *Proceedings of the National Academy of Sciences of the United States of America* **108**, 1645-1650 (2011).
2. A. Auger *et al.*, Efficient Delivery of Structurally Diverse Protein Cargo into Mammalian Cells by a Bacterial Toxin. *Mol Pharm* **12**, 2962-2971 (2015).

3. M. Drosten *et al.*, Genetic analysis of Ras signalling pathways in cell proliferation, migration and survival. *The EMBO journal* **29**, 1091-1104 (2010).
4. L. Thomer *et al.*, Antibodies against a secreted product of Staphylococcus aureus trigger phagocytic killing. *J Exp Med* **213**, 293-301 (2016).
5. M. Biancucci *et al.*, The bacterial Ras/Rap1 site-specific endopeptidase RRSP cleaves Ras through an atypical mechanism to disrupt Ras-ERK signaling. *Sci Signal* **11** (2018).
6. C. Guzman, M. Bagga, A. Kaur, J. Westermarck, D. Abankwa, ColonyArea: an ImageJ plugin to automatically quantify colony formation in clonogenic assays. *PloS one* **9**, e92444 (2014).
7. R. H. Shoemaker, The NCI60 human tumour cell line anticancer drug screen. *Nature reviews. Cancer* **6**, 813-823 (2006).
8. https://dtp.cancer.gov/discovery_development/nci-60/methodology.htm
9. D. P. Ivanov *et al.*, Multiplexing spheroid volume, resazurin and acid phosphatase viability assays for high-throughput screening of tumour spheroids and stem cell neurospheres. *PloS one* **9**, e103817 (2014).
10. V. Vidimar *et al.*, The AKT/BCL-2 Axis Mediates Survival of Uterine Leiomyoma in a Novel 3D Spheroid Model. *Endocrinology* **159**, 1453-1462 (2018).
11. W. C. Reinhold *et al.*, CellMiner: a web-based suite of genomic and pharmacologic tools to explore transcript and drug patterns in the NCI-60 cell line set. *Cancer research* **72**, 3499-3511 (2012).